

Select aspects of FEM analysis for bonded joints of polymer composite materials

A Rudawska

Department of Engineering Production, Lublin University of Technology,
Nadbystrzycka 36 Street, 20-618 Lublin, Poland

E-mail: a.rudawska@pollub.pl

Abstract. The paper presents selected aspects of modelling bonded joints of polymer composite materials by finite element method. The shear-loaded adhesive lap joints made of epoxy-graphite and epoxy-glass composite materials were investigated. The research objective was to determine correct modelling of adhesive layers using cohesive elements and of bonded joints for selected epoxy composite materials with different mechanical properties (e.g. Young's modulus) and geometrical dimensions, using, however, the same type of adhesive. The numerical analysis was performed based on experimental tests. A comparison is made between the distribution of reduced stress in the examined joint models according to the H-M-H hypothesis and that determined according to the maximum principal stress hypothesis. The finite elements analysis was performed in ABAQUS software and the traction-separation failure criterion was used for the damage onset and growth in the adhesive layer.

1. Introduction

Composite materials can be joining in a variety of ways and then used to produce numerous structural components [1,2]. One of such joining methods is adhesive bonding. The bonding technology offers numerous benefits, including the possibility of bonding various structural materials that have different properties and geometrical dimensions. When investigating adhesive joints, it is vital that both design and experimental tests be supplemented by finite element method based numerical analysis [3-5]. Such analysis is very useful at the design stage as it allows for simulating joint behaviour under various types of external load [6-8]. The application of numerical analysis to the investigation of adhesive joints also allows the determination of stress distributions in an adhesive layer [9] as well as indication of crucial structure elements that require special attention at the stage of their design or operation [10]. As a result, it is possible then to introduce some changes, e.g. to dimensions and shape of the given structure as well as the manner and location of applied load [11-14]. The application of FEM to design an adhesive joint allows both prompt verification of this adhesive joint and optimization of the above-mentioned parameters of such joint [15].

Some issues of FEM analysis of bonded composites joints are presented in some articles [16-17]. Pinto et al. [1] investigated the carbon-epoxy structures in repairing aspects used finite element stress analysis. Ashcroft et al. [18] conducted the analysis of the effect of environment on the fatigue of bonded composite joints. Finite element analysis is used to develop fatigue threshold prediction procedure. Madani et al. [19] analysed by finite element method the single- and double-sided composite repairs designed to reduce the concentration of the stresses at circular notches and cracks.



2. Experimental

2.1. Samples preparation

The object of the experiments concerned bonded single-lap joints of epoxy-graphite and epoxy-glass composite materials. A geometrical model of the examined joints is shown in figure 1.

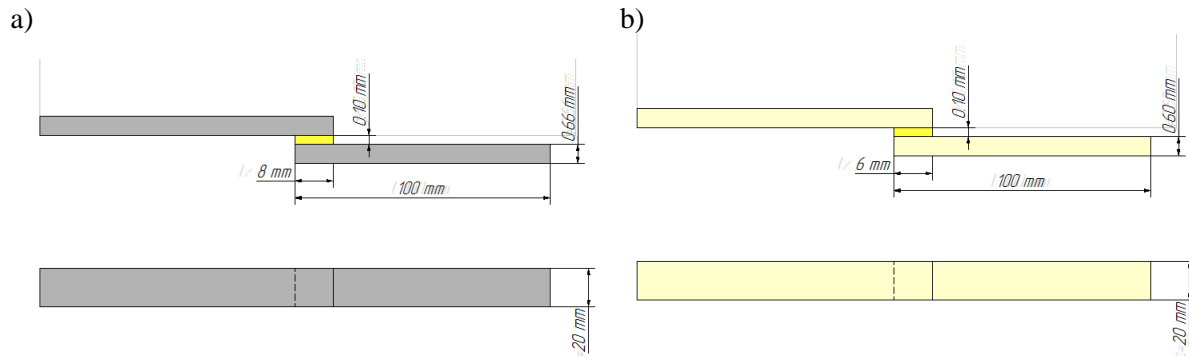


Figure 1. Geometrical model of joints: a) epoxy-graphite composite, b) epoxy-glass composite.

The samples were made of epoxy-graphite and epoxy-glass composite materials. The epoxy-graphite composite material was made of two layers of graphite fabric designated as GR-EP 199-45-003; the layer configuration applied was [0/90]. These were autoclave cured at $175 \pm 5^\circ\text{C}$ for 60 min. The thickness of the composite obtained was 0.66 ± 0.04 mm. The lap joint length was set equal to 8 mm (between 7.82 mm and 8.43 mm). The epoxy-glass composite material was made of two layers of glass fabric designated as glass laminate 3200-7781; the layer configuration applied was [0/90]. These were autoclave cured at 132°C for 60 min. The composite had a thickness of 0.60 ± 0.03 mm. The thickness of the adhesive layer was 0.10 ± 0.025 . The lap joint length was set equal to 6 mm (between 5.63 mm do 6.51 mm).

2.2. Experimental conditions

Bonded joints were made under the following experimental conditions:

- 1) surface preparation: degreasing with acetone-based degreasing agent Loctite7063,
- 2) adhesive: a two-component epoxy Loctite Fast Epoxy 3430,
- 3) curing conditions: [temperature \$20 \pm 2^\circ\text{C}\$](#) , curing time 48 h, load 0.02 MPa.

The degreasing operation is described in the study [20], while the adhesive characteristic is given in the paper [21]. Strength tests were undertaken to determine both failure force and strength of shear-loaded single-lap joints. The tests were performed using a Zwick Roell 150 testing machine, in compliance with DIN EN 1465 [22].

3. Numerical analysis

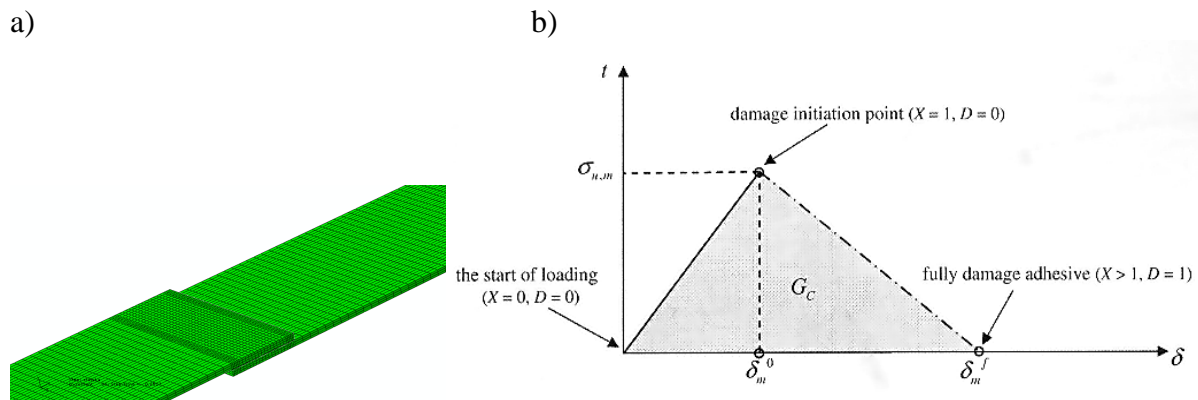
3.1. Numerical model

Based on the geometrical model of adhesive joints used in the experiments (Fig. 1), a numerical model of adhesive joints was developed. To model the adherends, 8-noded solid elements were used, with three translational degrees of freedom each. The adhesive layer was modelled with COH3D8 [23] cohesive finite elements that enabled the description of adhesive layer failure in the loading process of the adhesive joints. The mechanical properties of the composites used in the analyses were those supplied by the manufacturer and are shown in table 1.

A schematic of the numerical model is illustrated in figure 2a. Taking into account the data included in the studies, finite element mesh refinement in the vicinity of adhesive layer edges was applied, as it is there where sudden stress gradients can be expected to occur [24].

Table 1. Mechanical properties of tested composites.

Composite	Young modulus, MPa	Poisons ratio
Epoxy-graphite composite	140 000	0.26
Epoxy-glass composite	39 000	0.25

**Figure 2.** a) The part of the numerical model for examined adhesive joints, b) Traction-separation failure criterion used to describe the adhesive layer [26].

The boundary conditions of the numerical model were defined by means of blocking the translational degrees of freedom of the nodes located on the front surface of the upper sheet and leaving the possibility of displacement for the front surface of the lower steel only in the direction of applied load.

3.2. Failure criterion

The application of cohesive elements in the meshing process for adhesive layers requires that material with failure mechanism be defined. Figure 2b shows a material model of the adhesive used in the FEM analysis whose characteristics with failure initiation description included and evolution until complete loss of element rigidity based on the traction-separation law were defined. The cohesive zone model (figure 2b), combines a strength-based failure criterion to predict the damage initiation and fracture mechanics-based criterion to determine the damage propagation [25]. The same model the fatigue damage in adhesive bonded joints is presented by some research, e.g. Khoramishad et al. [11]. In addition to that, there exist numerous models of the traction-separation failure criterion that are described in the studies: (e.g. Pinto et al [1], De Moura et al. [25], Zadpoor et al. [26], Campilho et al. [27], Abdel Wahab et. Al [28]. Khoramishad et al. [11].

4. Test results

4.1. Experimental results

The conducted experimental tests enabled the determination of failure force considered basic for verifying the numerical analysis performed.

Table 2. Experimental results.

The type of joints	Failure force, N	Standard deviation, N	Strength, MPa
Epoxy-graphite composite	2875	287	17.97
Epoxy-glass composite	1838	331	15.33

Table 2 lists, among others, the results of failure force obtained in the experiments. The results presented are an average value of 10 measurements. The failure force value listed in table 2 was used to model load in a numerical model of adhesive joints for epoxy-graphite and epoxy-glass composite materials.

4.2. Numerical analysis results

4.2.1. Stress distribution. The presented numerical analysis results concern both adhesive joints and adhesive layers. As for the adhesive joints, the values and distributions of reduced stresses were determined according to the Huber-Mises-Hencky (H-M-H) strength hypothesis; while the results obtained for adhesive layers were determined using both the H-M-H strength hypothesis [11] and maximum principal stress hypothesis [18]. In many works [16,29] the maximum principal stresses as well as two principal stress components: S33 (peel stress) and S13 (shear stress) were analysed. Based on the numerical analysis performed, the value of failure load for adhesive joints was determined.

4.2.2. Stress distribution – epoxy/graphite composite. An example of the reduced stress distribution in bonded joints of the epoxy-graphite composite near the lap joint is shown in figure 3 a. In these numerical models there is one adhesive layer which was modelled cohesive finite elements. The nodes along lap joints lengths applied to the adhesive layer which it is joining to the samples.

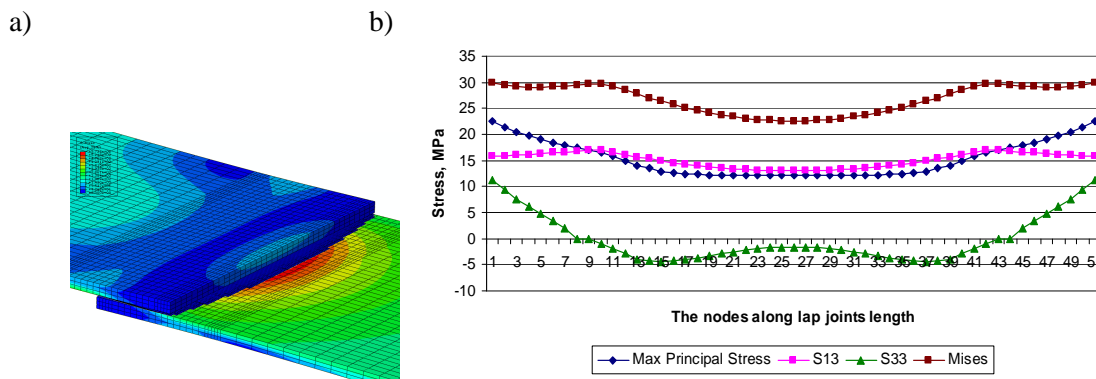


Figure 3. Bonded joints of epoxy-graphite composite: a) the reduced stress distribution, b) the stress distribution along lap joint length

The numerical results obtained for the adhesive layer are presented for one of the stages of adhesive layer failure, i.e. the initial failure process for which the highest value of maximum principal stress was obtained. Employing the maximum principal stress hypothesis, results were obtained for both maximum principal stress and principal stress components: S33 and S13. These components denoting peel stress and shear stress, respectively. The results are listed in Table 3 together with values of the stress components in general adhesive layer effort.

Table 3. Numerically obtained values of stresses in adhesively bonded joints of epoxy-graphite composite.

The type of stress	Maximum principal stress, MPa	S33, MPa	S13, MPa
Value	26.63	17.10	16.94

Examining epoxy graphite composite joints, it was observed that values of the peel stress (S33) and of the shear stress (S13) are similar. For the same stage of adhesive layer failure the value of reduced stress determined according to the Huber-Mises-Hencky hypothesis was 32.46 MPa.

It can be observed that a higher stress value is obtained if the Huber-Mises-Hencky reduced stress hypothesis ($\sigma_z = 32.46$ MPa) is employed. Therefore, it can be concluded that the application of the maximum principal stress hypothesis enables better evaluation of the load-bearing capacity of adhesive joints, defined as the maximum load value at which the joint fails. The distributions of the examined stresses along the lap joint length are shown in figure 3b.

According to the Goland and Reissner theory [9,30,31], the maximum principal stress in an adhesive lap joint occurs on the adhesive layer edges, and its value can be calculated using the relationship mentioned, among others, in the study. Shown in figure 3b, the distributions of maximum principal stress for the subsequent stages of adhesive layer loading are confirmed by the results of previous research [9,20,30] undertaken to investigate the character of stress distributions in adhesive joints. The presence of maximum principal stress along the adhesive layer edge and its very low values in the central region of the adhesive lap joint (figure 3b) prove the concentration of stress on the adhesive layer edges. It can also be noted that shear stresses prevail in the central region of the adhesive layer, while peel stresses do not occur there at all (which is proved by the negative values shown in figure 3b).

Based on the charts given in figure 3b, it can be claimed that both peel and shear stresses are vital at the initial stage of adhesive layer failure, these stresses being concentrated on the edges (peel stresses) and near the edges (shear stresses). In the central region of the lap joint, shear stresses play a dominant role over peel stresses.

4.2.3. Stress distribution - epoxy/glass composite. An example of the distributions of reduced stress in adhesively bonded joints of the epoxy-glass composite in the region of the lap joint is presented in figure 4a.

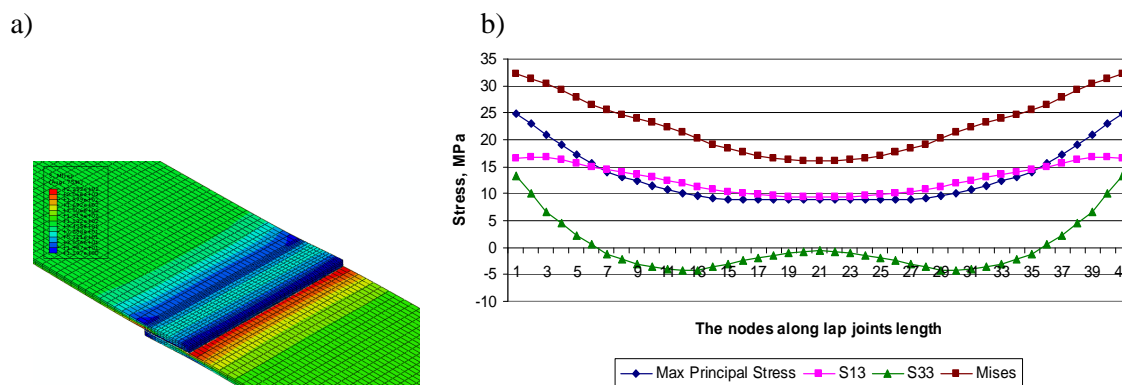


Figure 4. Bonded joints of epoxy-glass composite: a) the reduced stress distribution, b) the stress distribution along lap joint

Table 4 lists the values of maximum principal stress and principal stress components: S33 and S13 that describe peel stress and shear stress, respectively.

Table 4. Numerically obtained values of stresses in bonded joints of epoxy-glass composite.

The type of stress	Maximum principal stress, MPa	S33, MPa	S13, MPa
Value	29.74	20.19	16.93

In the case of the epoxy-glass composite joints, the value of peel stress (S33) is higher than that of shear stress (S13). This stress value can characterize the way in which adhesive joints of these composites fail. During the experimental failure tests, adhesive and cohesive adhesive layer failures were observed. This may result from similar values of the shear and peel stresses.

Comparing the values of reduced stress and maximum principal stress, it can be observed that a higher value stress was obtained using the Huber-Mises-Hencky hypothesis for reduced stress ($\sigma_z = 35.50$ MPa). In effect of the application of the hypothesis for maximum principal stress, it is possible to obtain values of components of this stress. As a result, a more thorough analysis of the stress state in adhesive layers can be performed. The distributions of stresses examined along the lap joint length are presented in figure 4b.

With the adhesively bonded joints of the epoxy-glass composite, the distributions of the examined stress types are of a similar character – the highest values occur on the adhesive layer edges, while much lower values are present in the central region of the adhesive layer. Examining the distributions of shear and peel stresses, it can clearly be observed that the values of these stresses on the adhesive layer edges are similar; however, the shear stresses (S_{13}) prevail in the central region of the adhesive layer. This can mean that both the shear and peel stresses are active at the beginning of the failure process, with the shear stresses taking on the leading role later on in the course of the process.

The visualisation of peel stress and its distribution along lap joints length of epoxy-glass composite joints in vector form are presented in figure 8.

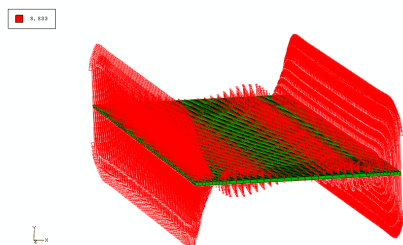


Figure 8. The visualisation of peel stress along lap joints length of epoxy-glass composite joints.

The distribution of the peel stress (figure 8) confirming the character of distribution which is presented in figure 7. In figure 8 it can be observed this character but in figure 7 it can be obtained the values of stress. In many cases the visualisation of stress distribution is very helpful to quick analysis of proper applied of boundary condition.

4.2.4. Comparison of stress distribution. A comparison of the stress distribution along the lap joint length for the epoxy-graphite and epoxy-glass composite is presented in figure 9 and figure 10.

It was observed (figure 9a) that higher maximum principal stress values were obtained for the adhesively bonded joint of the epoxy-glass composite characterized by a shorter lap joint length. These stresses have lower values in the central region along the lap joint length for the epoxy-glass composite material. The principal stress distribution in the adhesive joints of the epoxy-graphite composite is less varied than that for the epoxy-glass composite joints.

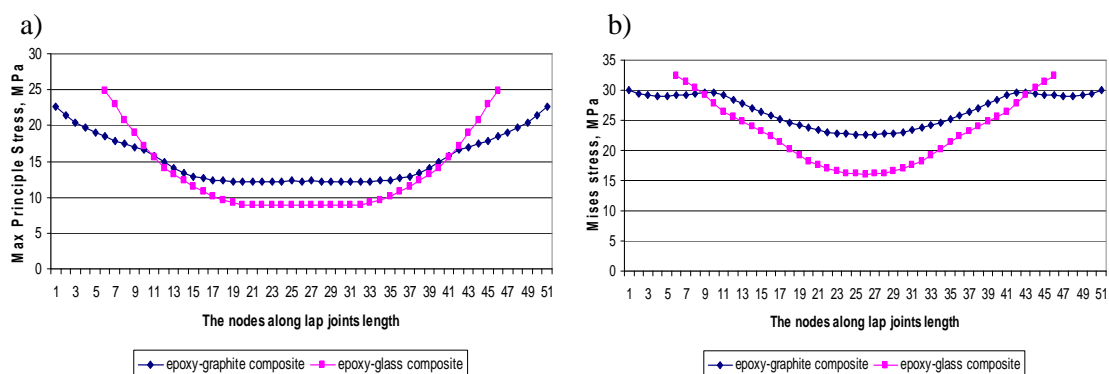


Figure 9. Distribution of: a) maximum principal, b) reduced stresses along lap joint length for epoxy-graphite and epoxy-glass composite bonded joints.

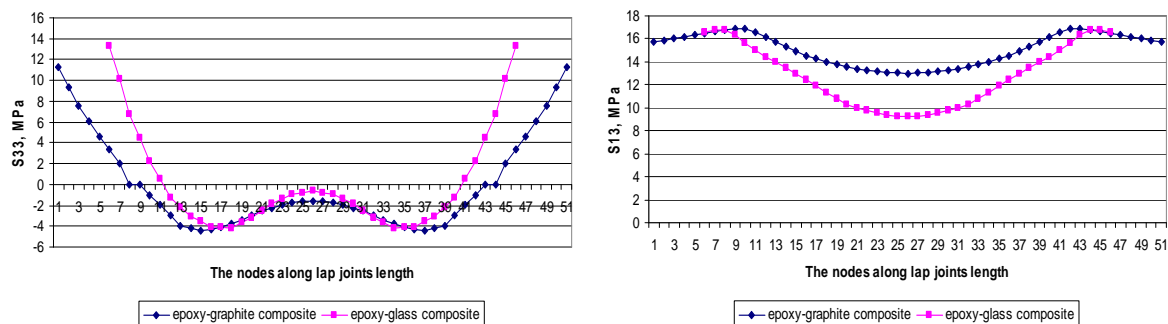


Figure 10. Distribution of: a) peel stresses b) shear stress along lap joint length for epoxy-graphite and epoxy-glass composite bonded joints.

Comparing the distributions of peel stresses (figure 10a) in the adhesive layer for both examined joints, it was observed that these distributions are quite similar in terms of both their values and characteristics. The distribution and values of the shear stress on the adhesive layer edges are the same. Differences occur in the central region of the lap joint length and they pertain to stress values. Lower values of the shear stress were obtained for the epoxy-glass composite joints with a value of Young's modulus lower by three times.

The differences in the distributions of reduced stresses can be observed on both the adhesive layer edges and in the centre of the lap. The differences exist in the values and character of the stress distribution. As for the epoxy-glass composite material, it was observed that maximum values of these stresses occur on the lap joint edge, accompanied by a gradual decrease in the value of this stress progressing from the adhesive layer edge. Furthermore, equal values of reduced stress on much a shorter length of the lap in its central region than is the case with epoxy-graphite composite joints. It can be observed that the decrease in reduced stresses occurs at some distance from the lap edge and the variation in stress is less dramatic than is the case with the epoxy-graphite composite.

4.3. Comparison of the experimental and numerical results

Table 5 lists the values of failure forces obtained in the experiments and numerical analysis for the following polymer composite materials: epoxy-glass and epoxy-graphite.

Table 5. Values of adhesive failure force obtained in the experiments and numerical analysis for bonded joints of polymer composites.

Composite	Failure force, N	
	Experimental test	Numerical analysis
Epoxy-graphite composite	2875	2555
Epoxy-glass composite	1838	1796

Comparing the results for the selected polymer composite materials listed in table 5, it can be observed that the experimental and numerical results compare quite well. The result agreement for the epoxy-glass composite adhesive joint was approx. 98%. In effect of a comparative analysis of the experimental and numerical results for the adhesively bonded joints of the epoxy-graphite composite, a certain difference in failure load can be observed: the failure load value obtained in the experiment is $P = 2875$ N, while the FEM-calculated load value is $P = 2555$ N. The agreement of the results in this case amounts to 89%. The difference in the failure load values obtained can result from the assumptions made in the modelling of adhesive joints and also the different properties of the adherends. The higher the tensile rigidity of the adherends, the higher the value of the force that causes adhesive joint failure.

5. Conclusions

Comparing the results obtained in the numerical analysis with those obtained in the experiments, it can be claimed that the numerical model of the tested joint agrees well with the real joint, given the simplified assumptions taken in modelling and confidence intervals for the experiments. The higher the tensile rigidity of the adherends, the higher the value of the force that causes adhesive joint failure, which accords with the Volkersen theory.

Using numerical analysis, it is possible to obtain the distributions of stresses based on various strength hypotheses, which at the same time allows a more detailed evaluation of adhesive joint effort. It is observed that the concentration of stresses occurs on adhesive layer edges. The distributions of shear and peel stresses on the adhesive layer edges are similar; however, it should be noted that the shear stresses (S_{13}) prevail in the central region of the adhesive layer. This can mean that at the beginning of the failure process both the shear and peel stresses are active, with the former taking on the leading role later on in the course of the process.

Owing to different properties of the adherends (including Young's modulus), the obtained distributions of stresses are varied. The material with a higher modulus (epoxy-graphite composite) is exhibited higher values of stresses in the central region along the lap joint length. In contrast, the less rigid material (with a lower Young's modulus) is characterized by more dramatic variations in the stresses along the lap joint length. These results confirm the effect of mechanical properties on the distributions and values of stresses.

References

- [1] Pinto A M G, Campilho R D S G, de Moura M F S F and Mendes I R 2010 *Int. J. Fatigue* **30** 329
- [2] Gude M R, Prolongo S G, Gomez-del Rio T and Urena A 2011 *Int. J. Adhes. Adhes.* **31** 695
- [3] He X 2011 *Int. J. Adhes. Adhes.* **31** 248
- [4] Aydin M D, Özel A and Temiz S 2004 *J. Adhes. Sci. Technol.* **18** 1589
- [5] Ávila A F and de O. Bueno P 2004 *Int. J. Adhes. Adhes.* **24** 407
- [6] Pironi A and Nicoletto G 2004 *Eng. Frac. Mech.* **71** 859
- [7] Liljedahl C D M, Crocombe A D, Wahab M A and Ashcroft I A 2007 *Int. J. Adhes. Adhes.* **27** 505
- [8] Khalili S M R, Khalili S, Pirouzhshemi M R, Shokuhfar A and Mittal R K 2008 *Int. J. Adhes. Adhes.* **28** 411
- [9] Castagnetti D and Dragoni E 2009 *Int. J. Adhes. Adhes.* **29** 125
- [10] Diaz Diaz A, Hadj-Ahmed R, Foret G and Ehrlacher A 2009 *Int. J. Adhes. Adhes.* **29** 67
- [11] Khoramishad H, Crocombe A D, Katnam K B and Ashcroft I A 2010 *Int. J. Fatigue* **32** 1146
- [12] Magalhães A G, de Moura M F S F and Gonçalves J P M 2005 *Int. J. Adhes. Adhes.* **25** 313
- [13] Gcoin A, Lestriez P, Assih J, Objois A and Delmas Y 2009 *Int. J. Adhes. Adhes.* **29** 572
- [14] Apalak M K and Engin A 2004 *J. Adhes. Sci. Technol.* **18** 529
- [15] You M, Yan Z-M, Zheng X-L, Yu H-Z and Li Z 2007 *Int. J. Adhes. Adhes.* **27** 696
- [16] Taib A A, Boukhili R, Achiou S, Gordon S and Boukehili H 2006 *Int. J. Adhes. Adhes.* **26** 226
- [17] Wahab M A, Ashcroft I A, Crocombe A D and Smith P A 2004 *Composites A* **35** 213
- [18] Ashcroft I A, Wahab M A, Crocombe A D, Hughes D J and Shaw S J 2001 *Composites A* **32** 45
- [19] Madani K, Touzain S, Feaugas X, Benguediab M and Ratwani M 2009 *Int. J. Adhes. Adhes.* **29** 225
- [20] Rudawska A 2010 *Int. J. Adhes. Adhes.* **30** 574
- [21] Rudawska A 2013 *Selected issues of constitutional processes of homogeneous and hybrid adhesion joints* (Lublin: Publisher University of Lublin)
- [22] Standard DIN EN 1465. Adhesives. Determination of tensile lap-shear strength of bonded joints.
- [23] Abaqus 6.9 – Documentation 2009
- [24] de Moraes A B, Pereira A B, Teixeira J P and Cavaleiro N C 2007 *Int. J. Adhes. Adhes.* **27** 679

- [25] de Moura M F S F, Concalves J P M, Chousal J A G and Campilho R D S G 2008 *Int. J. Adhes. Adhes.* **28** 419
- [26] Zadpoor A A, Sinke J and Benedictus R 2009 *Int. J. Adhes. Adhes.* **29** 558
- [27] Campilho R D S G, de Moura M F S F, Ramantani D A, Morais J J L and Domingues J J M S 2009 *Int. J. Adhes. Adhes.* **29** 678
- [28] Wahab M A, Hilmy I, Ashcroft I A and Crocombe A D 2010 *J. Adhes. Sci. Technol.* **24** 325
- [29] Wahab M A, Crocombe A D, Beevers A and Ebtehaj K 2002 *Int. J. Adhes. Adhes.* **22** 61
- [30] Adams R D, Comyn J and Wake W C 1997 *Structural Adhesive Joints in Engineering* (London: Chapman and Hall)
- [31] Godzimirski J 2002 *The strength of constructional bonding joints* (Warsaw: WNT)